Received: 5 August 2024 | Revised: 3 September 2024 | Accepted: 7 October 2024

DOI: 10.1096/fj.202401807R

RESEARCH ARTICLE

The FASEB Journal

# The expression of intestinal Cyp2c55 is regulated by the microbiota and inflammation

**Adrian Hilman**[1,2] | **Tetsu Sato**[1] | **Bambang Dwi Wijatniko**[1,3] | **So Fujimura**[1] | **Katsushi Nakamura**[1] | **Hiroto Miura**[4] | **Ken Iwatsuki**[5] | **Ryo Inoue**[4] | **Takuya Suzuki**[1]

[1]Graduate School of Integrated Sciences for Life, Hiroshima University, Higashi-Hiroshima, Japan

[2]Department of Food Technology, Faculty of Agriculture, Universitas Sumatera Utara, Medan, Indonesia

[3]Department of Food and Agricultural Product Technology, Universitas Gadjah Mada, Yogyakarta, Indonesia

[4]Faculty of Agriculture, Setsunan University, Hirakata, Japan

[5]Faculty of Applied Bioscience, Tokyo University of Agriculture, Tokyo, Japan

**Correspondence**
Takuya Suzuki, Graduate School of Integrated Sciences for Life, Hiroshima University, 1-4-4 Kagamiyama, Higashi-Hiroshima 739-8528, Japan.
Email: takuya@hiroshima-u.ac.jp

**Funding information**
MEXT | Japan Society for the Promotion of Science (JSPS), Grant/Award Number: 22H03512; Tojuro Iijima Foundation for Food Science and Technology

## Abstract

Although the mutualistic relationship between the intestinal microbiota and the human host is crucial for maintaining health, the underlying mechanisms of this relationship remain unclear. In the present study, aiming to elucidate the regulatory mechanisms governing the Cyp2c55 expression, which is predominantly observed in colonic tissues, germ-free, antibiotic-administered and colitic mice, as well as mouse colonoids, were used as experimental models. RNA sequencing showed comparable decreases in the colonic Cyp2c55 expression in germ-free and antibiotic-administered mice, when compared with that in specific pathogen-free mice. Furthermore, administration of dextran sulfate sodium decreased the Cyp2c55 expression in colitic mice. For these mice, a Pearson correlation analysis also showed a positive correlation between the Cyp2c55 expression and unconjugated bile acids (BAs), including chenodeoxycholic, muricholic, deoxycholic, lithocholic, and ursodeoxycholic acids, as well as taurine (T)-conjugated secondary BAs, including deoxycholic acid. Moreover, bacterial genera, such as *Muribaculaceae* and unclassified *Lachnospiraceae*, also exhibited a positive correlation with these BAs. While administration of an agonist of the pregnane X receptor (PXR) increased the Cyp2c55 expression in mouse colonoids, inflammatory cytokines decreased it. In conclusion, Cyp2c55 was highly expressed in the colonic epithelial cells of mice in a microbiota-dependent manner. The

**Abbreviations:** ASVs, amplicon sequence variants; BA, bile acid; BSH, bile salt hydrolase; CA, cholic acid; CAR, constitutive androstane receptor; CDCA, chenodeoxy cholic acid; Cyp2c, cytochrome P450 2C; DCA, deoxycholic acid; DSS, dextran sulfate sodium; FXR, farnesoid X receptor; Gapdh, glyceraldehyde-3-phosphate dehydrogenase; HCA, hyocholic acid; HDCA, hyodeoxycholic acid; HETE, hydroxyeicosatetraenoic acid; IBD, inflammatory bowel disease; LCA, lithocholic acid; MCA, muricholic acid; Oaz1, ornithine decarboxylase antizyme 1; OTU, operational Taxonomic Unit; PBAs, primary BAs; PCN, pregnenolone 16α-carbonitrile; PCoA, Principal coordinates analysis; PXR, pregnane X receptor; QIIME, Quantitative Insights into Microbial Ecology; qRT-PCR, quantitative reverse transcription-polymerase chain reaction; Rps28, ribosomal protein S28; SBAs, secondary bile acids; SEPP, SATé-enabled phylogenetic placement; SPF, specific pathogen-free; TPM, transcripts per million; UDCA, ursodeoxycholic acid; VDR, vitamin D receptor.

Adrian Hilman and Tetsu Sato equally contributed to this work.

underlying mechanism seemed to involve a BA-mediated PXR activation. In addition, the colonic expression of Cyp2c55 was regulated by the inflammatory response. Although the physiological function of Cyp2c55 remains largely unidentified, our findings suggested that Cyp2c55 may play a role in the mutualistic interaction between the intestinal microbiota and the intestinal homeostasis.

**KEYWORDS**

bile acid, Cyp2c55, intestinal inflammation, intestinal microbiota

## 1 | INTRODUCTION

The mutualistic relationship between the intestinal microbiota and the human host is crucial for maintaining health and avoiding disease development.[1] The intestinal microbiota is involved in processes such as the digestion of complex carbohydrates and the synthesis of essential vitamins. It also protects the host against pathogens and modulates the immune system. This mutualistic relationship is sustained by adaptive changes in the intestinal gene expression, which promotes an optimal environment for both the microbial and the host's functions.[2] Abnormal changes in the intestinal gene expression can disrupt this relationship, resulting in dysbiosis. Accumulating evidence demonstrates that dysbiosis is closely linked to intestinal diseases such as the inflammatory bowel diseases (IBDs) and the irritable bowel syndrome, metabolic disorders such as obesity and diabetes, and mental health issues involving the gut–brain axis.[3,4] Therefore, an understanding of the molecular mechanisms underlying the mutualistic relationship between the intestinal microbiota and the human host may result in potential therapeutic avenues for the treatment of various diseases.

The intestinal microbiota influences the gene expression in intestinal tissues through various molecular mechanisms. One significant mechanism involves the secondary bile acids (SBAs) produced by the intestinal microbiota.[5] To facilitate lipid digestion and absorption, primary BAs (PBAs) such as the taurine (T)-conjugated cholic acid (CA) and the chenodeoxycholic acid (CDCA) are synthesized in the hepatocytes and released into the duodenum. Small portions of PBAs (~5%) escape into the colon, where the microbiota converts them to SBAs, such as the deoxycholic acid (DCA) and the lithocholic acid (LCA).[6] These SBAs interact with nuclear receptors including the pregnane X receptor (PXR), the constitutive androstane receptor (CAR), the vitamin D receptor (VDR), the Farnesoid X receptor (FXR), and other signaling pathways in the host. These interactions lead to changes in the gene expression that can affect the intestinal homeostasis and the immune response.[7] For example, the SBAs, including the isoDCA, are involved in the homeostasis of regulatory T cells via FXR, which are essential for maintaining immune tolerance and preventing excessive inflammatory responses.[8] However, the physiological roles of the intestinal microbiota and the BAs are not fully understood.

The cytochrome P450 2C (Cyp2c) family, a part of the Cyp superfamily, plays crucial roles in the metabolism of both endogenous and exogenous compounds. These enzymes are largely involved in the oxidative metabolism of approximately 20% of clinically used drugs, including nonsteroidal anti-inflammatory drugs, anti-convulsants, and anti-hypertensive agents.[9] Polyunsaturated fatty acids such as the arachidonic and the linoleic acids, which are present in cell membranes, also undergo NADH-dependent oxidation by certain Cyp2c enzymes. For example, in an in vitro assay, it was reported that that mouse Cyp2c55, a homolog of human Cyp2c18, metabolized arachidonic acid mainly to an eicosanoid, the 19-hydroxyeicosatetraenoic acid (HETE).[10] Previous studies showed that the HETEs are involved in the regulation of several physiological functions, such as the vascular tone, the ion transport, the intestinal barrier, and the inflammatory reaction.[11,12]

The tissue expression patterns of the Cyp2c members exhibit considerable variation among isoforms. This variation is closely related to the bioactivity and the regulation of the expression of each isoform. A previous study demonstrated that Cyp2c55 is highly expressed in the mouse intestinal tissues, particularly the large intestine, where a large number of microorganisms inhabit.[13] This information suggests that Cyp2c55 may be important for regulating intestinal functions and maintaining the mutualistic relationship between the intestinal microbiota and the host. Furthermore, it has been reported that, in mice, the hepatic Cyp2c55 expression is regulated by nuclear receptors CAR and PXR.[14] However, the physiological roles of Cyp2c55 and the mechanisms regulating its expression in the intestine remain largely uncharacterized.

The present study aimed to investigate the molecular mechanisms of the mutualistic relationship between the intestinal microbiota and the host. In particular, we focused on the regulation of the colonic Cyp2c55 expression, because a whole transcriptome analysis by RNA sequencing showed that the *Cyp2c55* expression was depleted in

the colons of germ-free mice, but not in specific pathogen-free (SPF) mice. In addition, the regulation of Cyp2c55 expression was examined in antibiotic-treated and dextran sulfate sodium (DSS)-induced colitic mice, as well as in mouse colonoids.

## 2 | MATERIALS AND METHODS

### 2.1 | Mice

All animal studies were pre-approved by the Animal Care Committee of the Hiroshima University (approval no. C22-44-2). Mice were maintained in accordance with the Guidelines for the Care and Use of Laboratory Animals at Hiroshima University, the National Research Council's Guide for the Care and Use of Laboratory Animals, and the ARRIVE guidelines. Seven-week-old male ICR germ-free and SPF mice were purchased from SLC Japan (Hamamatsu, Japan). Seven-week-old male C57BL/6J mice were purchased from Charles River Laboratories Japan (Yokohama, Japan). Mice were housed under the following conditions throughout the experiment: controlled temperature (22 ± 2°C), relative humidity (40–60%), and lighting (lights on 8:00–20:00). Mice were allowed to acclimate to the laboratory environment and had free access to an AIN-93G formula diet and tap water for at least a week. At the end of the experiments, mice were euthanized via exsanguination under isoflurane anesthesia.

### 2.2 | Experimental design

Four studies (Experiments 1–4) were conducted to investigate the regulation of the intestinal Cyp2c55 expression.

In Experiment 1, the gene expression profiles in the colons of germ-free and SPF mice were examined. Total RNA was extracted from colonic tissues of the germ-free and SPF mice by NucleoSpin RNA (Macherey-Nagel, Düren, Germany), according to the manufacturer's instructions, and subjected to whole transcriptome and quantitative reverse transcription-polymerase chain reaction (qRT-PCR) analyses, as described below. Colonic tissues were also subjected to immunoblot and immunofluorescence analyses. Cecal contents were subjected to BA analysis. Total RNA extracted from different intestinal segments (duodena, jejuna, ilea, ceca, proximal colons, and distal colons) and livers of SPF mice were subjected to qRT-PCR analysis.

In Experiment 2, the Cyp2c55 expression was examined in the colons of mice administered with antibiotics with different antibacterial spectra. After acclimatization, mice ($n = 35$) were randomly allocated to (1) control, (2) cocktail, (3) vancomycin, (4) polymyxin B, and (5) neomycin groups. The cocktail group was administered via drinking water a cocktail of 3 antibiotics [250 mg/L vancomycin sulfate, 100 mg/L polymyxin B sulfate, and 250 mg/L neomycin sulfate (Fujifilm Wako Pure Chemical)]. The doses of the antibiotics were based on preliminary experiments carried out at these premises. Mice in the vancomycin, polymyxin B, and neomycin groups were administered the respective antibiotics. The control group was administered ultrapure water. All treatments were administered for 21 days. All mice were fed the AIN-93G formula diet throughout the experimental period. Colonic tissues were subjected to qRT-PCR, immunoblot, and HETEs analyses as described below. Cecal samples were collected and subjected to BA and microflora analyses as described below.

In Experiment 3, the Cyp2c55 expression was examined in the colons of DSS-induced colitic mice. Mice ($n = 28$) were randomly allocated to (1) control, (2) DSS_5d, (3) DSS_7d, and (4) DSS_9d groups. The DSS_5d, DSS_7d, and DSS_9d groups were administered via drinking water 2% (w/v) DSS (MP Biomedicals, Santa Ana, CA, USA) for 5, 7, and 9 days, respectively, and were euthanized. The control group was administered ultrapure water for 9 days. The body weights of mice were measured daily. To evaluate the severity of colitis, the clinical score was evaluated daily using a standard scoring system[15] (Table S1). After measuring the length of the colons of mice, the colonic tissues were subjected to qRT-PCR and immunoblot analyses as described below. Fecal samples were collected one day prior to dissection and subjected to BA and microflora analyses.

In Experiment 4, the Cyp2c55 expression in mouse colonoids was examined. Mouse colonoids were generated as previously described,[16] with slight modifications. Crypts were isolated by collagenase dissociation and Percoll separation, embedded in Matrigel (Corning, Corning, NY, USA), and overlaid with growth media [advanced Dulbecco's modified Eagle medium/F12 supplemented with 10% R-spondin conditioned medium (Merck, Rahway, NJ, USA), 5% Noggin conditioned medium, 2% NS supplement (Fujifilm Wako Pure Chemical), 1% N2 supplement (Fujifilm Wako Pure Chemical), 1 mM N-acetyl-L-cysteine, 0.5 nM Wnt Surrogate-Fc fusion recombinant protein (Thermo Fisher Scientific, Waltham, MA, USA), 50 ng/mL murine EGF (PeproTech, Cranbury, NJ, USA), and 10 μM Y-27632 (Selleck Chemicals, Houston, TX, USA)]. Noggin-expressing 293 T cells were kindly provided by Dr. Hans Clevers (Hubrecht Institute, Utrecht, Netherlands). Cultures were depleted with Y-27632 two days post-seeding and passaged every 7–10 days. Media

was changed every two days. For the experiments, the colonoids were differentiated in growth media without Y-27632 or Wnt protein for four days from the third day post-seeding. Mouse colonoids were treated with agonists of PXR (pregnenolone 16α-carbonitrile; PCN; Cayman, Ann Arbor, MI, USA), CAR (1, 4-bis[2-(3, 5-dichloropyridyloxy)]benzene; TCPOBOP, Cayman), and VDR (calcitriol, Fujifilm Wako Pure Chemical) for 24 h, and a cytokine mix (TNF-α, IFN-γ, and IL-1β) for 48 h.

## 2.3 | Whole transcriptome analysis of the mouse colon (Experiment 1)

Total RNA was extracted from the colonic tissues of germ-free and SPF mice using NucleoSpin RNA (Macherey-Nagel, Düren, Germany), according to the manufacturer's instructions. Six samples of each group were pooled and processed as previously described.[17] The mapped read counts were normalized to transcripts per million (TPM). After adding 1, the TPM values were $Log_2$ transformed and used to generate a scatter plot and calculate the fold change.

## 2.4 | qRT-PCR analysis (Experiments 1–4)

Total RNA was extracted from mouse tissues and colonoids using NucleoSpin RNA and Sepasol®-RNA I Super G (Nacalai Tesque, Kyoto, Japan) and reverse-transcribed to cDNA using a ReverTra Ace qPCR RT kit (TOYOBO, Osaka, Japan), according to the manufacturer's instructions. The qRT-PCR analysis was conducted using the 2× Brilliant III Ultra-Fast SYBR Green QPCR Master Mix (Agilent Technologies, Santa Clara, CA, USA) in a StepOne Real-Time PCR System (Thermo Fisher Scientific). The primer sequences are shown in Table S2. The mRNA expression of target genes was calculated by the $2^{-\Delta\Delta Ct}$ method with ribosomal protein S28 (*Rps28*), glyceraldehyde-3-phosphate dehydrogenase (*Gapdh*), and ornithine decarboxylase antizyme 1 (*Oaz1*) as the reference genes.

## 2.5 | Immunoblot analysis (Experiments 1–4)

Using a Polytron homogenizer (KINEMATICA, Luzern, Switzerland), mouse colonic tissues and colonoids were homogenized in 400 and 80 μL, respectively, of a lysis buffer [1% (w/v) SDS, 1% (v/v) Triton X-100, and 1% (w/v) sodium deoxycholate in 30 mM Tris with protease and phosphatase inhibitors (pH 7.4)]. Protein concentrations were then determined using a Protein Assay BCA kit (Nacalai Tesque). Next, the protein extracts were mixed with half a volume of Laemmli sample buffer [6% (w/v) SDS, 30% (v/v) glycerol, 15% (v/v) β-mercaptoethanol, and 0.02% (w/v) bromophenol blue in 188 mM Tris, (pH 6.8)] and heated to 95°C for 10 min. Proteins (20 μg) were separated by SDS-PAGE and transferred to polyvinylidene fluoride membranes. After visualizing the total protein content using Ponceau S staining, the membranes were blocked with skim milk and incubated first with the corresponding primary antibodies and then with peroxidase-conjugated anti-rabbit and anti-mouse IgGs. Detailed information on the antibodies used in the experiments is shown in Table S3. The blots were developed by an enhanced chemiluminescence method (Western Lightning Plus-ECL, PerkinElmer, Waltham, MA, USA) using an Amersham Imager 680 apparatus (Cytiva, Marlborough, MA, USA).

## 2.6 | Immunofluorescence (Experiment 1)

The colonic tissues of germ-free and SPF mice were embedded in an Optimal Cutting Temperature compound (Sakura Finetek, Tokyo, Japan). The cryosections (8 μm thickness) prepared on slide glasses were blocked with 5% normal goat serum and incubated with rabbit anti-Cyp2c55 at 4°C for 16 h. Afterward, the samples were incubated for 1 h with Alexa Fluor 488-conjugated anti-rabbit IgG and DAPI. Detailed information on the antibodies used in the experiment is shown in Table S3. The specimens were preserved in a mounting fluid, and the fluorescence was visualized with a Leica FW4000 fluorescence microscope (Leica Microsystems, Wetzlar, Germany).

## 2.7 | Cecal and fecal BA analysis (Experiments 2 and 3)

CA, CDCA, α-muricholic acid (MCA), β-MCA, ω-MCA, hyocholic acid (HCA), hyodeoxycholic acid (HDCA), LCA, ursodeoxycholic acid (UDCA), and taurine (T)-conjugated secondary forms in mouse ceca (Experiment 2) and feces (Experiment 3) were quantified as previously described with minor modifications.[18] Briefly, the cecal contents and feces were freeze-dried and the BAs were extracted using methanol. Nordeoxycholic acid was used as the internal standard. BAs present in the extracts were analyzed by ultraperformance liquid chromatography–mass spectrometry (Waters, Milford, MA, USA).

### 2.8 | HETE analysis (Experiments 2 and 3)

The HETEs (5-, 12-, 15-, 19-, and 20-HETEs) in the mouse colonic tissues were quantified as previously described with minor modifications.[19] Briefly, the colonic tissues (30 mg) were homogenized in 10 volumes of PBS using a Polytron homogenizer (KINEMATICA). The HETEs present in the homogenates were extracted with ethyl acetate, dried under a continuous nitrogen gas flow, and reconstituted with isopropanol. The HETEs in the resultant samples were analyzed by ultraperformance liquid chromatography–mass spectrometry (Waters).

### 2.9 | Metagenomic analysis of 16S rRNA genes in the intestinal microbiota (Experiments 2 and 3)

Bacterial DNA in the mouse cecal contents (Experiment 2) and feces (Experiment 3) was isolated with a Quickgene QuickGene SP kit (KURABO, Osaka, Japan) and a NucleoSpin DNA Stool kit (Macherey-Nagel), according to the manufacturer's instructions. Library preparation for analysis using an Illumina MiSeq Next Generation Sequencer (Illumina, San Diego, CA, USA) was carried out as previously described.[20] PCR amplification of the 16S rRNA V3-V4 regions (460 bp) was conducted using primers 314F and 805R.[21] Sequence data were analyzed using Quantitative Insights into Microbial Ecology (QIIME) 2 (ver. 2021.11 and 2023.2), with denoising using the DADA2 plugin. Amplicon sequence variants (ASVs) were defined, and their taxonomy was classified by the sklearn-classifier against the SILVA database (138; 99% Operational Taxonomic Units (OTUs), full-length sequences). In the present study, we removed singletons and ASVs assigned to mitochondria and chloroplasts. Subsequently, a phylogenetic tree was generated using the SATé-enabled phylogenetic placement (SEPP).

### 2.10 | Statistical analysis

Data are shown as the mean ± the SEM. Statistical analyses were carried out using JMP Pro 16.2.0 (SAS Institute Inc., Cary, NC, USA). The two-tailed unpaired Student's t-test was used for comparison of two groups (Experiment 1). Tukey–Kramer post hoc and Steel–Dwass tests were used for comparisons of multiple groups (Experiments 1–4). Values were considered statistically significant if $p < .05$.

## 3 | RESULTS

### 3.1 | Dependence of the Cyp2c55 expression on the presence of intestinal microbiota

We hypothesized that certain genes, which are upregulated by the presence of the intestinal microbiota, played important roles in the mutualistic relationship between the intestinal microbiota and the host. In Experiment 1, to find such genes, a whole transcriptome analysis of the colonic tissues of germ-free and SPF mice was conducted. Of the total 17 598 genes detected in germ-free and SPF mice, 480 were upregulated and 1342 were downregulated greater than 2-fold in germ-free mice, when compared with those in SPF mice (Figure 1A). Among the downregulated genes, 8 genes (*Amn, Ang4*, *Cyp2c55*, *Hp*, *Nr1h5*, *Mettl7a2*, *Mettl7a3*, and *Slc30a10*) were abundantly expressed in SPF mice (TPM >10) and obviously reduced in germ-free mice (fold change <0.2) (Table S4). Due to the information on the physiological roles of *Cyp2c55* is scarce when compared with other genes, and the TPM of *Cyp2c55* was the highest among the 8 genes, we focused on *Cyp2c55*. Moreover, among 15 members of the Cyp2c subfamily, only Cyp2c55 was clearly downregulated in the colons of germ-free mice (Figure 1B), suggesting a possible crucial role in the mutualistic relationship between the intestinal microbiotas and the hosts. The qRT-PCR and immunoblot analyses also confirmed the drastic downregulation of the Cyp2c55 expression in germ-free mice (Figure 1C,D). In the lower segments of the intestines of SPF mice, such as ceca and colons, which are densely colonized by intestinal microorganisms, *Cyp2c55* expression was higher than in the upper intestinal segments, such as duodena, jejuna, and ilea (Figure 1E). Interestingly, the hepatic Cyp2c55 expression was much lower than that observed in all intestinal segments. Immunofluorescence demonstrated that Cy2c55 was highly expressed in the luminal surface of the epithelial cells (Figure 1F). These results indicated that the intestinal Cyp2c55 expression greatly depended on the presence of the intestinal microbiota and that it possibly has an important role in the maintenance of the intestinal homeostasis.

### 3.2 | Involvement of the BA metabolism in the colonic Cyp2c55 expression

A previous study showed that the colonic Cyp2c55 expression was possibly regulated by LCA.[22] Therefore, in the present work, the cecal BAs in germ-free and SPF mice were determined by mass spectrometry. The taurine (T)-conjugated PBAs produced in the liver are

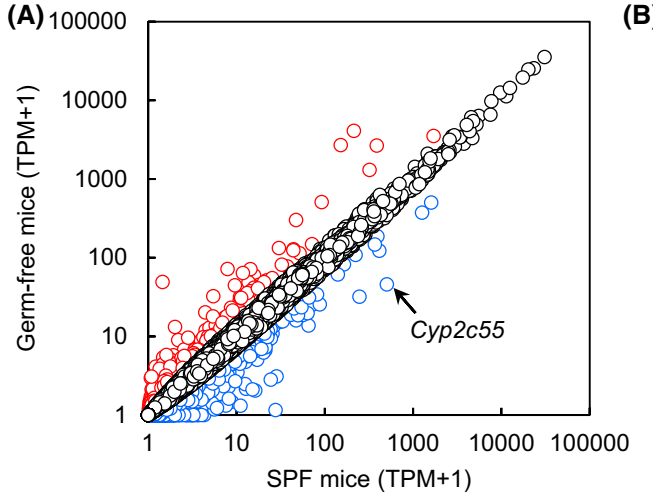


(B)

| NCBI accession | Gene symbol | SPF | GF | Fold change |
|---|---|---|---|---|
| NM_001001446 | Cyp2c23 | 2.1 | 1.4 | 0.76 |
| NM_007815 | Cyp2c29 | 0.0 | 0.0 | 1.03 |
| NM_010001 | Cyp2c37 | 0.0 | 0.0 | 1.00 |
| NM_010002 | Cyp2c38 | 0.0 | 0.0 | 1.00 |
| NM_010003 | Cyp2c39 | 0.0 | 0.0 | 1.00 |
| NM_010004 | Cyp2c40 | 6.3 | 4.1 | 0.70 |
| NM_001167875 | Cyp2c50 | 0.0 | 0.0 | 1.00 |
| NM_206537 | Cyp2c54 | 0.0 | 0.0 | 1.00 |
| NM_028089 | Cyp2c55 | 503.5 | 44.7 | 0.09 |
| NM_028191 | Cyp2c65 | 6.4 | 4.0 | 0.68 |
| NM_001011707 | Cyp2c66 | 0.3 | 0.0 | 0.75 |
| NM_001024719 | Cyp2c67 | 10.8 | 11.0 | 1.01 |
| NM_001039555 | Cyp2c68 | 114.5 | 104.1 | 0.91 |
| NM_001104525 | Cyp2c69 | 8.4 | 7.4 | 0.89 |
| NM_145499 | Cyp2c70 | 0.1 | 2.1 | 2.82 |

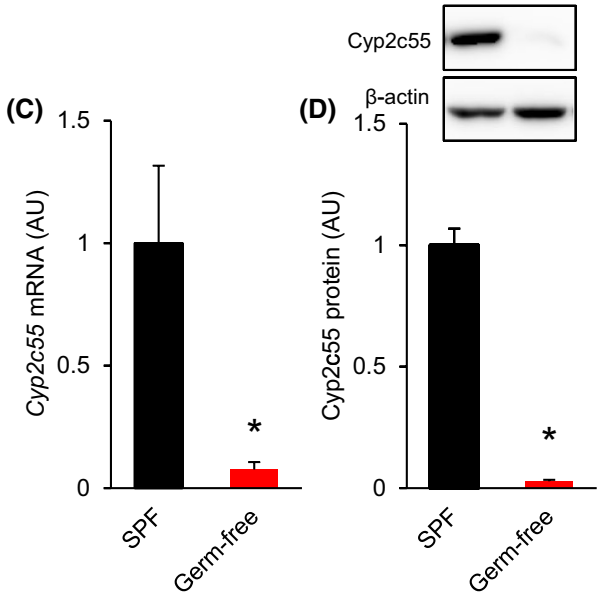


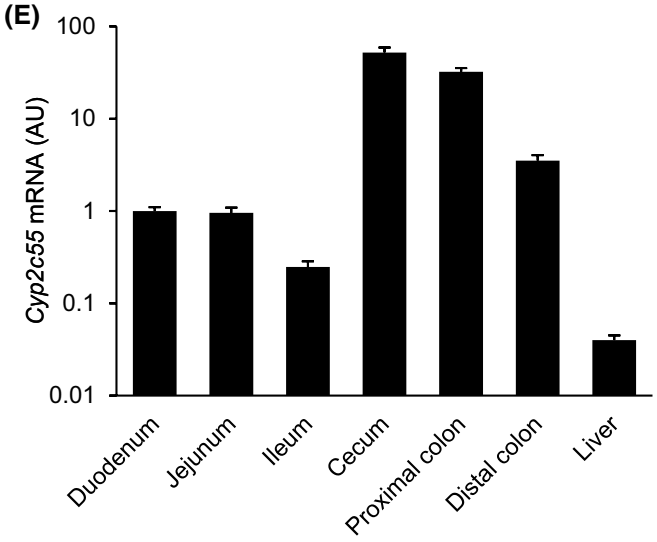


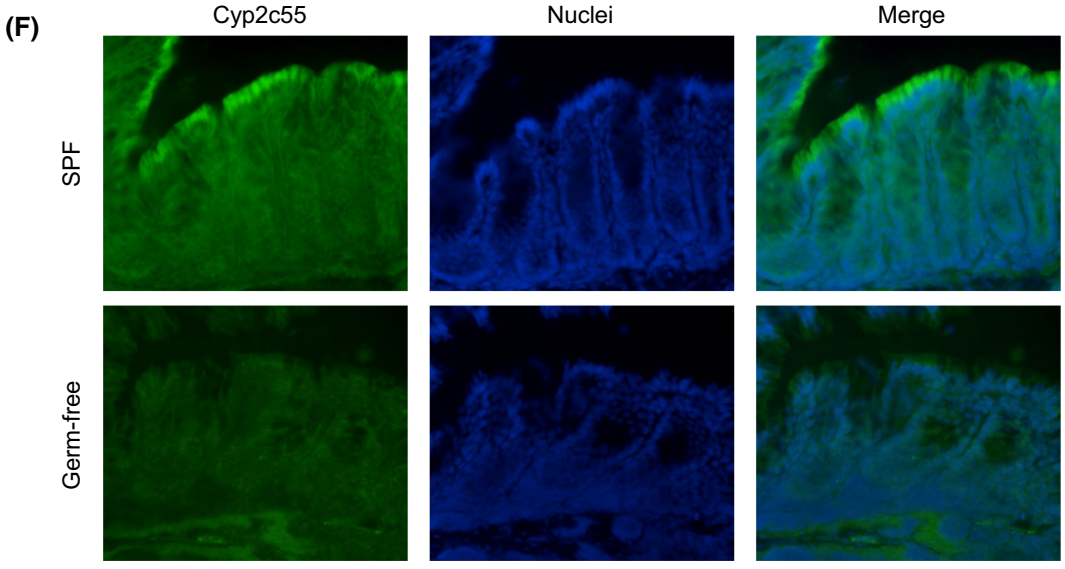

**FIGURE 1** Dependence of the Cyp2c55 expression on the intestinal microbiota. (A–C) Total RNA from the colon of germ-free (GF) and specific pathogen-free (SPF) mice was subjected to RNA sequencing (A, B) and qRT-PCR (C) analyses. Data (transcripts per million, TPM) were $Log_2$ transformed after adding 1 to the TPMs, and a scatter plot was generated (A). The plots colored red and blue indicate genes with upregulation and downregulation greater than 2-fold, respectively. TPMs and fold changes of Cyp2c subfamily members are shown (B). (D) The Cyp2c55 protein expression in the colon of germ-free and SPF mice was determined by an immunoblot analysis. (E) The Cyp2c55 mRNA expression in the different intestinal segments and liver was determined by qRT-PCR analysis. (F) The Cyp2c55 protein in the colon of SPF mice was visualized by an immunofluorescence analysis. Data are shown as the mean ± the SEM; $n = 6$. Asterisks indicate significant differences when compared with SPF mice ($p < .05$).

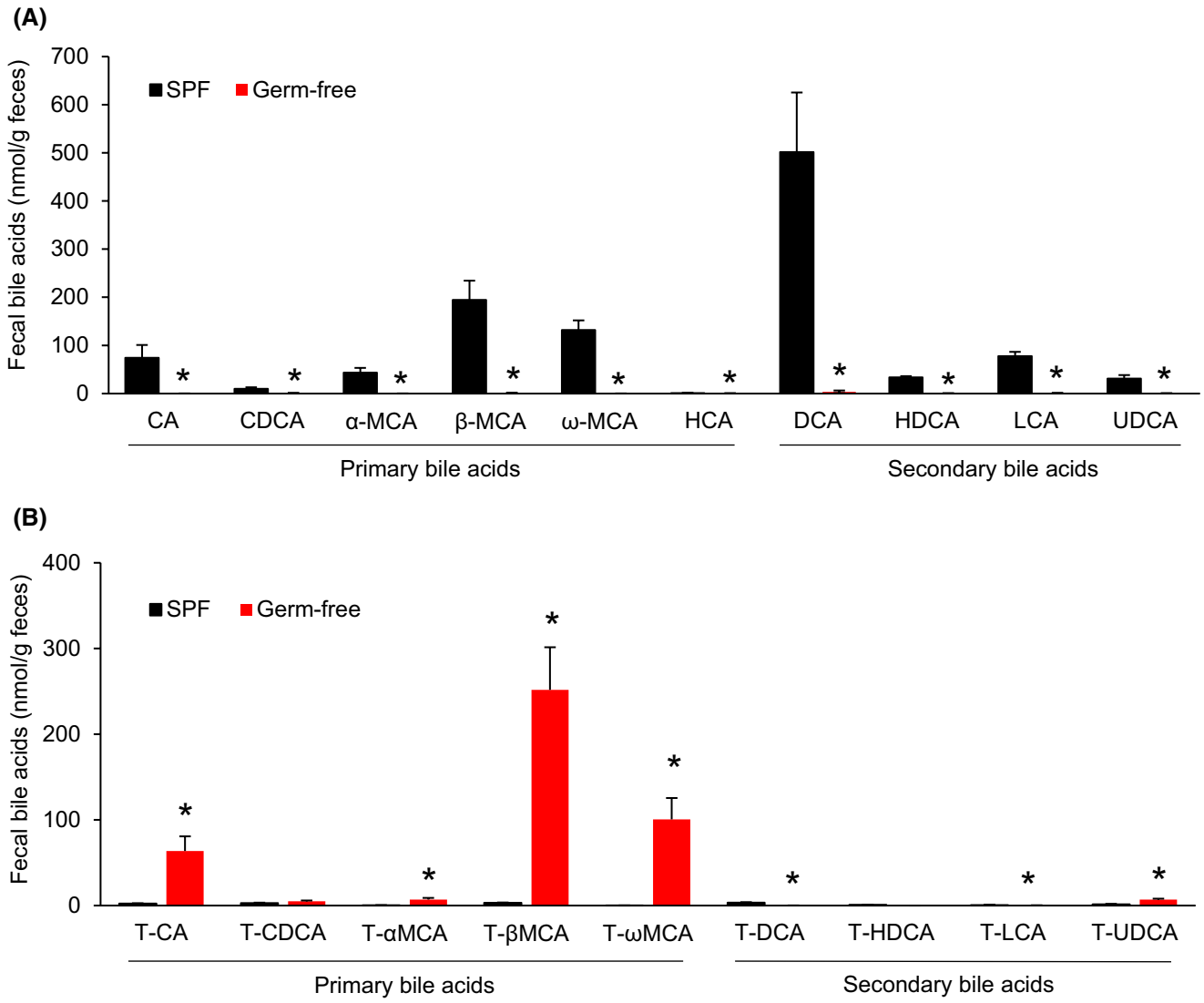


**FIGURE 2** Effect of the intestinal microbiota on the cecal composition of bile acids. (A, B) The concentrations of unconjugated (A) and taurine (T)-conjugated (B) bile acids in ceca of germ-free (GF) and specific pathogen-free (SPF) mice were measured using ultraperformance liquid chromatography–mass spectrometry. Data are presented as the mean ± the SEM; $n = 6$. Asterisks indicate significant differences when compared with the SPF mice ($p < .05$).

deconjugated and converted to SBAs by intestinal microorganisms. Accordingly, BAs present in the ceca of SPF mice were mostly deconjugated (Figure 2A,B). All deconjugated BAs measured in the ceca of SPF mice, including PBAs and SBAs, were higher than in germ-free mice. In contrast, except for T-DCA, T-HDCA, and T-LCA, taurine-conjugated BAs were higher in germ-free mice than those in SPF mice. A Spearman's rank correlation analysis showed that all unconjugated BAs and T-DCA positively correlated with the mRNA and protein levels of Cyp2c55 (Figure S1). These results also showed that the colonic Cyp2c55 expression depended on the presence of

the intestinal microbiota and may be involved in the BA metabolism.

### 3.3 | Involvement of vancomycin-sensitive bacteria in the Cyp2c55 expression

In Experiment 2, to further examine the involvement of the intestinal microflora and the BA metabolism in the colonic Cyp2c55 expression, mice were administered with antibiotics with different antibacterial spectra. Cyp2c55 mRNA and protein are naturally expressed at low levels in the colons of germ-free mice. The administration of the antibiotic cocktail (vancomycin, polymyxin B, and neomycin) also caused reductions in the Cyp2c55 mRNA and protein expressions in the colons of mice (Figure 3A,B). Vancomycin alone, but not polymyxin B or neomycin, also reduced the Cyp2c55 mRNA and protein expressions. The BA analysis showed that the antibiotic cocktail and vancomycin reduced all unconjugated PBAs and SBAs, although the reduction in CA was not statistically significant. Interestingly, neomycin, which did not affect the Cyp2c55 expression, reduced the SBAs, but not CA, α-MCA, or β-MCA. The T-CA and T-MCAs (α/β/ω) were higher in antibiotic-cocktail-administered and vancomycin-administered mice than in control mice. A Spearman's rank correlation analysis showed that all unconjugated BAs, T-DCA, and THDCA positively correlated with the mRNA and protein levels of colonic Cyp2c55. These results suggested that the reduction of Cyp2c55 expression by the antibiotic cocktail and vancomycin occurred by depletion of both PBAs and SBAs, whereas the Cyp2c55 expression in the neomycin-administered mice was maintained by unconjugated PBAs such as CA, α-MCA, and β-MCA.

### 3.4 | Antibiotics treatment affected the microflora profiles

In Experiment 2, antibiotics vancomycin, polymyxin B, and neomycin, which have different antimicrobial spectra, were employed. Vancomycin and polymyxin B generally target Gram-positive and Gram-negative bacteria, respectively. Neomycin, in contrast, exhibits a broad spectrum of activity against a variety of bacteria. The microflora analysis based on 16S rRNA genes showed that the antibiotic cocktail, vancomycin, and neomycin, but not polymyxin B, significantly reduced the α-diversity in the observed species and the Chao1 and the Shannon indices of the microbial community (Figure 4A–C). Principal coordinates analysis (PCoA) based on the Bray–Curtis, the weighted UniFrac, and the unweighted UniFrac distances showed that the administration of the antibiotic cocktail, vancomycin, and neomycin had a negative impact on the β-diversity of the microflora (Figure 4D–F). The clustering observed in these three groups was independent of that observed in the control group and the groups differed from each other. Figure 4G shows the effect of treatments on the relative abundances of observed phyla. While the antibiotic cocktail reduced Bacteroidota (one of the most dominant phyla) and Verrucomicrobiota, it increased Proteobacteria and Actinobacteriota. Vancomycin dramatically increased three phyla, Proteobacteria, Verrucomicrobiota, and Deferribacterota. Polymyxin B decreased Verrucomicrobiota. Neomycin reduced Firmicutes and increased Bacteroidota. At the genus level, 229 taxa were detected, and we initially extracted genera that had a relative abundance greater than 0.1% in the control group. For a better visualization, observed genera were grouped according to their relative abundances and divided as shown in Figure 4H,I. Figure 4H,I shows bacterial genera with relative abundances greater than 3% and 1%, respectively. Administration of the antibiotic cocktail resulted in a reduction of the majority of genera, with the exception of *Lactobacillus* and *Brevibacterium*, which remarkably increased. Vancomycin administration also decreased numerous genera, especially Gram-positive bacteria such as unclassified *Lachnospiraceae*, *Lachnospiraceae_NK4A136_group*, *Colidextribacter*, *Blautia*, unclassified *Oscilospiraceae*, unclassified *Peptococcaceae*, *Clostridia_UCG-014*, *Anaerotrunus*, *Intestinimonas*, *Acetatifactor*, *Dubosiella*, and uncultured *Lachnospiraceae*. While Gram-negative bacteria such as *Muribaculaceae*, *Bacteroides*, *Alistipes*, and *Oscillibacter* also decreased after the administration of vancomycin, some others such as *Akkermansia* and *Parasutterella* increased. Although the dose of polymyxin B used in the present study only caused moderate effects, it still decreased *Akkermansia*. Neomycin administration decreased several genera, such as *Lachnospiraceae_NK4A136_group*, *Blautia*, *Parasutterella*, *Lactobacillus*, uncultured *Peptococcaceae*, *Clostridia_UCG-014*, *Anaerotruncus*, *Intestinimonas*, *Acetatifactor*, and uncultured *Lachnospiraceae*. Figure S3 illustrates the remaining genera, many of which exhibited a decrease in abundance following the administration of the antibiotic cocktail, vancomycin, and neomycin. With the exception of *Akkermansia*, *Parasutterella*, *Brevibacterium*, *Clostridia_vadinBB60_group*, and *Lactobacillus*, a Spearman's rank correlation analysis showed that the mRNA and the protein expressions of Cyp2c55 positively correlated with several bacterial genera (Figure S4).

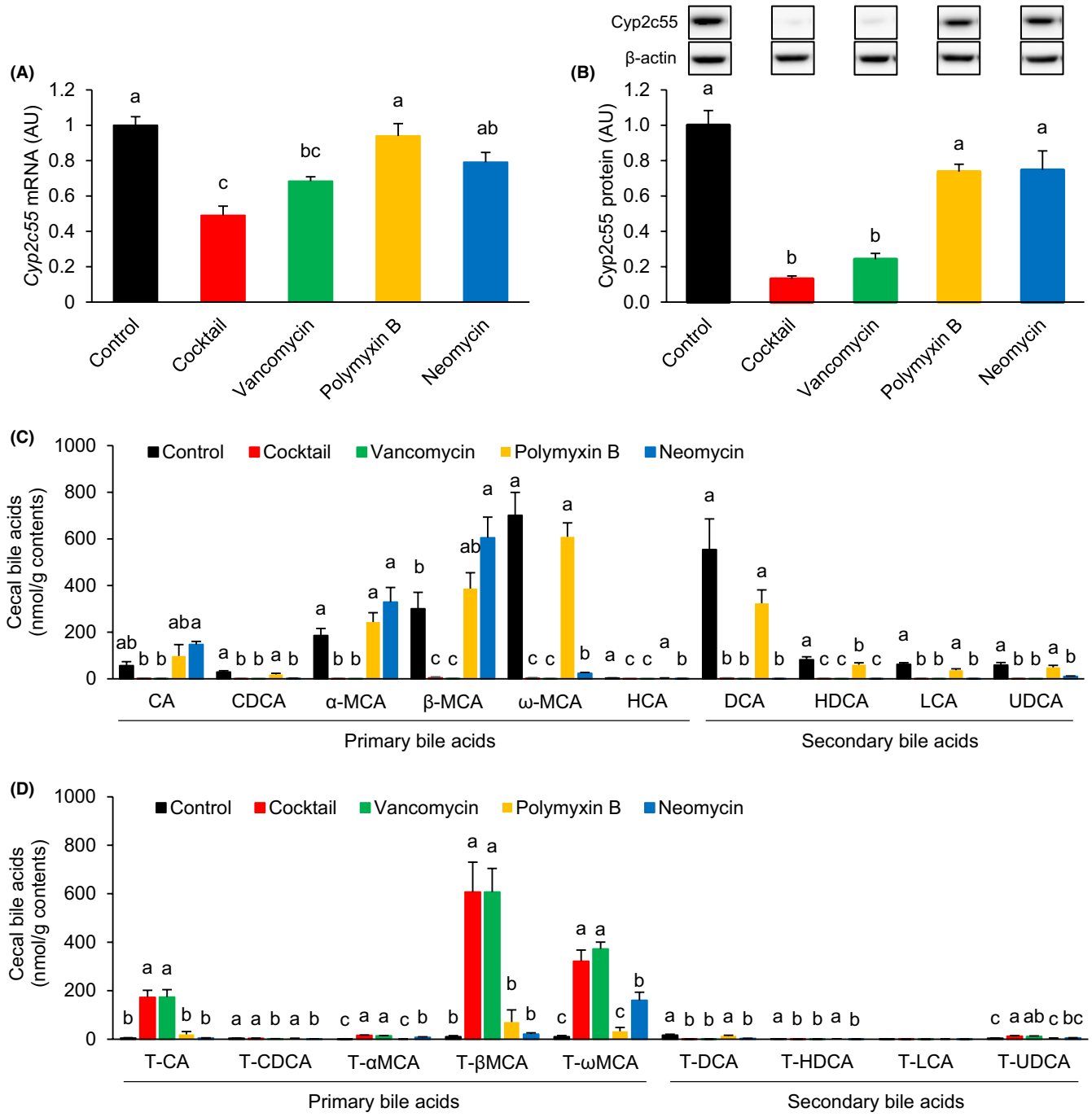


**FIGURE 3** Effect of the antibiotic treatments on the colonic Cyp2c55 expression and the fecal composition of bile acids. (A, B) The mRNA and the protein expressions of Cyp2c55 in the colon of mice administered with antibiotics cocktail and individual antibiotics (vancomycin, polymyxin B, and neomycin) were assessed by qRT-PCR (A) and immunoblot (B) analyses, respectively. (C, D) The concentrations of unconjugated (C) and taurine (T)-conjugated (D) bile acids (BAs) in feces of mice administered with an antibiotic cocktail and individually antibiotics were measured using ultraperformance liquid chromatography–mass spectrometry. Data are presented as the mean ± the SEM; $n = 7$. Mean values without a common letter are significantly different ($p < .05$).

## 3.5 | Effect of antibiotics on the HETE production in the colonic tissues

Although the physiological role of Cyp2c55 is largely unknown, our in vitro study demonstrated that Cyp2c55 mainly metabolized arachidonic acid to the 19-HETE. However, the 19-HETE levels in the colonic tissues of mice with and without antibiotics were under the detection limit (Figure S5). The other HETEs including the 5-, 12-, and 15-HETE were detected, but no differences were found between groups.

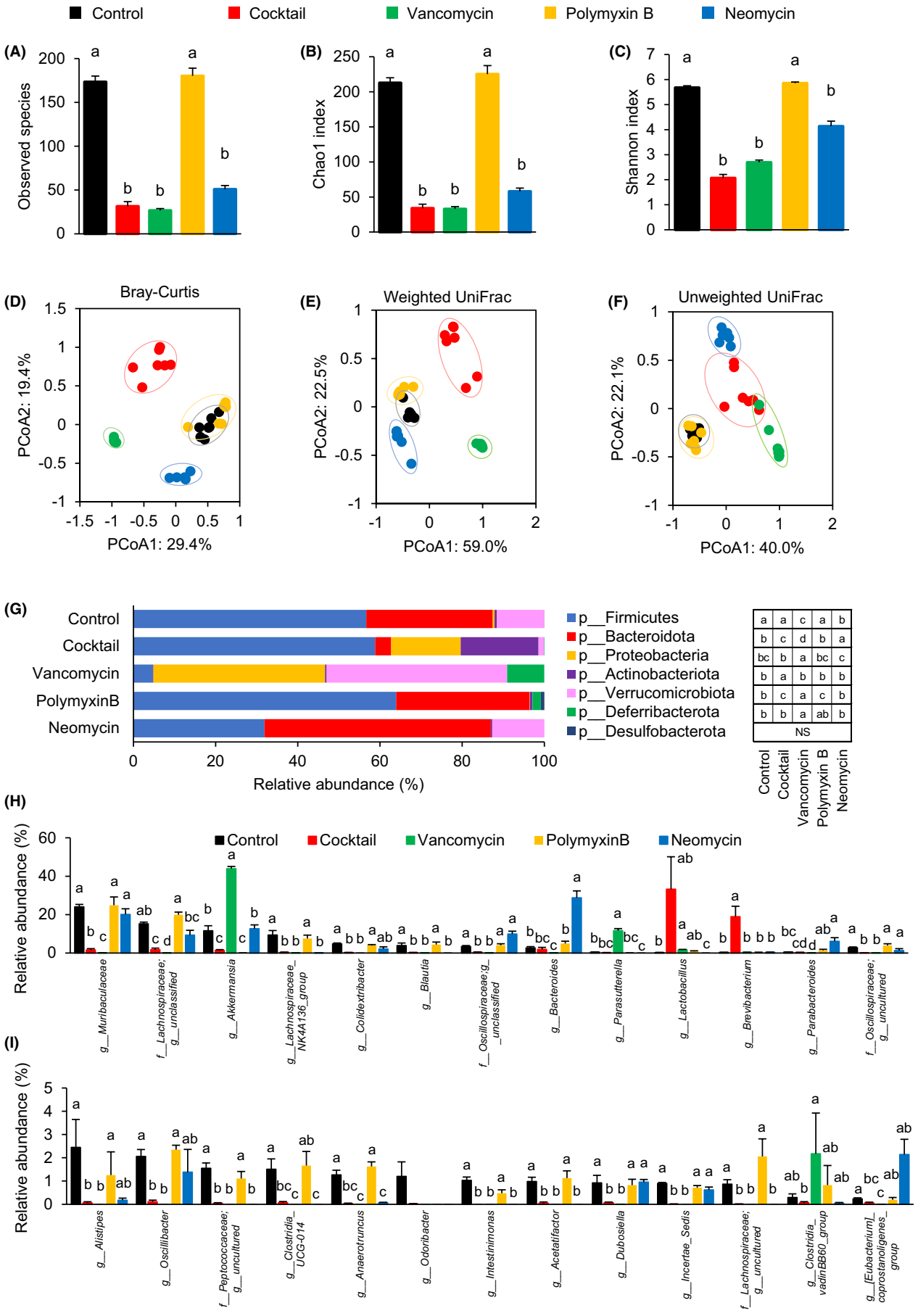
Control
Cocktail
Vancomycin
Polymyxin B
Neomycin
(A)
Observed species
(B)
Chao1 index
(C)
Shannon index
(D)
Bray-Curtis
PCoA2: 19.4%
PCoA1: 29.4%
(E)
Weighted UniFrac
PCoA2: 22.5%
PCoA1: 59.0%
(F)
Unweighted UniFrac
PCoA2: 22.1%
PCoA1: 40.0%
(G)
Control
Cocktail
Vancomycin
PolymyxinB
Neomycin
Relative abundance (%)
p__Firmicutes
p__Bacteroidota
p__Proteobacteria
p__Actinobacteriota
p__Verrucomicrobiota
p__Deferribacterota
p__Desulfobacterota
NS
(H)
Relative abundance (%)
g__Muribaculaceae
f__Lachnospiraceae;g__unclassified
g__Akkermansia
g__Lachnospiraceae_NK4A136_group
g__Colidextribacter
g__Blautia
f__Oscillospiraceae;g__unclassified
g__Bacteroides
g__Parasutterella
g__Lactobacillus
g__Brevibacterium
g__Parabacteroides
f__Oscillospiraceae;g__uncultured
(I)
Relative abundance (%)
g__Alistipes
g__Oscillibacter
f__Peptococcaceae;g__uncultured
g__Clostridia_UCG-014
g__Anaerotruncus
g__Odoribacter
g__Intestinimonas
g__Acetatifactor
g__Dubosiella
g__Incertae_Sedis
f__Lachnospiraceae;g__uncultured
g__Clostridia_vadinBB60_group
g__[Eubacterium]_coprostanoligenes_group

**FIGURE 4** Effect of antibiotic administration on the fecal microbiota composition. (A–I) The cecal microbiota of mice administered with an antibiotic cocktail and individual antibiotics (vancomycin, polymyxin B, and neomycin) were analyzed by 16S rRNA gene sequencing. The number of observed species (A), the Chao1 index (B), and the Shannon evenness (C) in the microbiota was calculated. Principal coordinate analysis plots of the fecal microbiotas were generated based on the Bray–Curtis (D), the weighted UniFrac (E), and the unweighted UniFrac (F) distances using QIIME2. The mean abundances of fecal microbiotas at the phylum level are shown (G). For a better visualization, genera were grouped and divided in those with abundances greater than 3% and 1%, respectively (H, I). Data are presented as the mean ± the SEM; $n = 7$. Mean values without a common letter are significantly different ($p < .05$).

## 3.6 | Downregulation of Cyp2c55 in colitic mice

The DSS-induced colitic mouse model has been extensively validated as a reliable representation of human ulcerative colitis. As expected, in Experiment 3, DSS administration resulted in the induction of colitis, which was evidenced by the observed increase in the clinical score and the colon shortening (Figure 5A,B). As with previous studies,[15,23] DSS administration resulted in the upregulation of the mRNA expression of inflammatory cytokines and chemokines, including *Tnf*, *Il1b*, *Il6*, *Cxcl1*, and *Cxcl5*. The mRNA levels of these cytokines in mice administered DSS for 5, 7, and 9 days were observed to be higher than those in control mice (Figure 5C–G). In contrast, following the commencement of DSS administration, the mRNA and protein expressions of Cyp2c55 exhibited a downward trend after 7 and 9 days, respectively (Figure 5H,I). In addition, the administration of DSS resulted in reductions of unconjugated PBAs and SBAs, as well as taurine-conjugated SBAs, which in turn led to increases in conjugated PBAs (Figure 6A,B). In mice administered DSS for 9 days, the levels of all unconjugated BAs (with the exception of CA) and taurine-conjugated SBAs (with the exception of T-LCA and T-UDCA) were found to be lower than those observed in control mice. With the exception of T-CDCA, taurine-conjugated PBAs exhibited higher levels in the DSS_9d group, when compared with control mice. Similar trends were observed in the DSS_5d and DSS_7d groups, although the changes in the levels of some BAs were non-statistically significant. A Spearman's rank correlation analysis demonstrated that, except for CA, all unconjugated BAs, as well as some taurine-conjugated BAs (e.g., T-CDCA, T-DCA, and T-HDCA), exhibited a positive correlation with either or both the mRNA and the protein expressions of Cyp2c55 (Figure S6).

## 3.7 | DSS administration affected the intestinal microbiota composition

The administration of DSS for 5, 7, and 9 days decreased the α-diversity of the fecal microbiota, as indicated by the reductions found in the observed species and the Chao1 and Shannon indices. However, reductions in the Chao1 index in the DSS_7d and DSS_9d groups were non-statistically significant (Figure 7A–C). PCoA based on the Bray–Curtis, the weighted UniFrac, and the unweighted UniFrac distances showed that DSS administration affected the β-diversity of the microbiota, as indicated by the distinct clustering of the three DSS groups and the control group (Figure 7D–F). Based on the Bray–Curtis and the weighted UniFrac distances, distances between the three DSS groups and the control cluster were observed to be greater in the plots for the longer periods of DSS administration, suggesting a period-dependent alteration. At the phylum level, while DSS administration decreased the relative abundance of Firmicutes, it increased Proteobacteria, although a statistical difference was observed only 9 days post-administration (Figure 7G). At the genus level, 112 taxa were detected, and we initially extracted genera that had a relative abundance greater than 0.1% in the control group. For a better visualization, observed genera were grouped according to their relative abundances and divided as shown in Figure 7H,I. Figure 7H,I shows genera with relative abundances higher than 4 and 1%, respectively. While DSS administration for 5, 7, and 9 days decreased *Muribaculaceae*, unclassified and uncultured *Lachnospiraceae*, *Lachnospiraceae_NK4A136_group*, uncultured *Oscillospiraceae*, *Lachnoclostridium*, and *[Eubacterium]_coprostanoligenes_group*, it increased *Bacteroides*, *Escherichia_Shigella*, *Erysipelatoclostridium*, and *Enterococcus*, although some changes were non-statistically significant. The *Parabacteroides* genus was higher in the DSS_5d group than in the other groups. Figure S7 shows genera with a relative abundance lower than 1% in all groups. While DSS administration decreased some genera such as uncultured *Ruminococcaceae*, *Roseburia*, *Incertae_Sedis*, and *[Eubacterium]_brachy_group*, it increased genera *ASF356* and unclassified *Oscillospirales*, although some changes were not statistically significant. A Spearman's rank correlation analysis showed that some genera including *Muribaculacea*, unclassified *Lachnospiraceae*, *Blautia*, *Lachnoclostridium*, and *Roseburia* correlated with both the mRNA and the protein expression of Cyp2c55 (Figure S8).

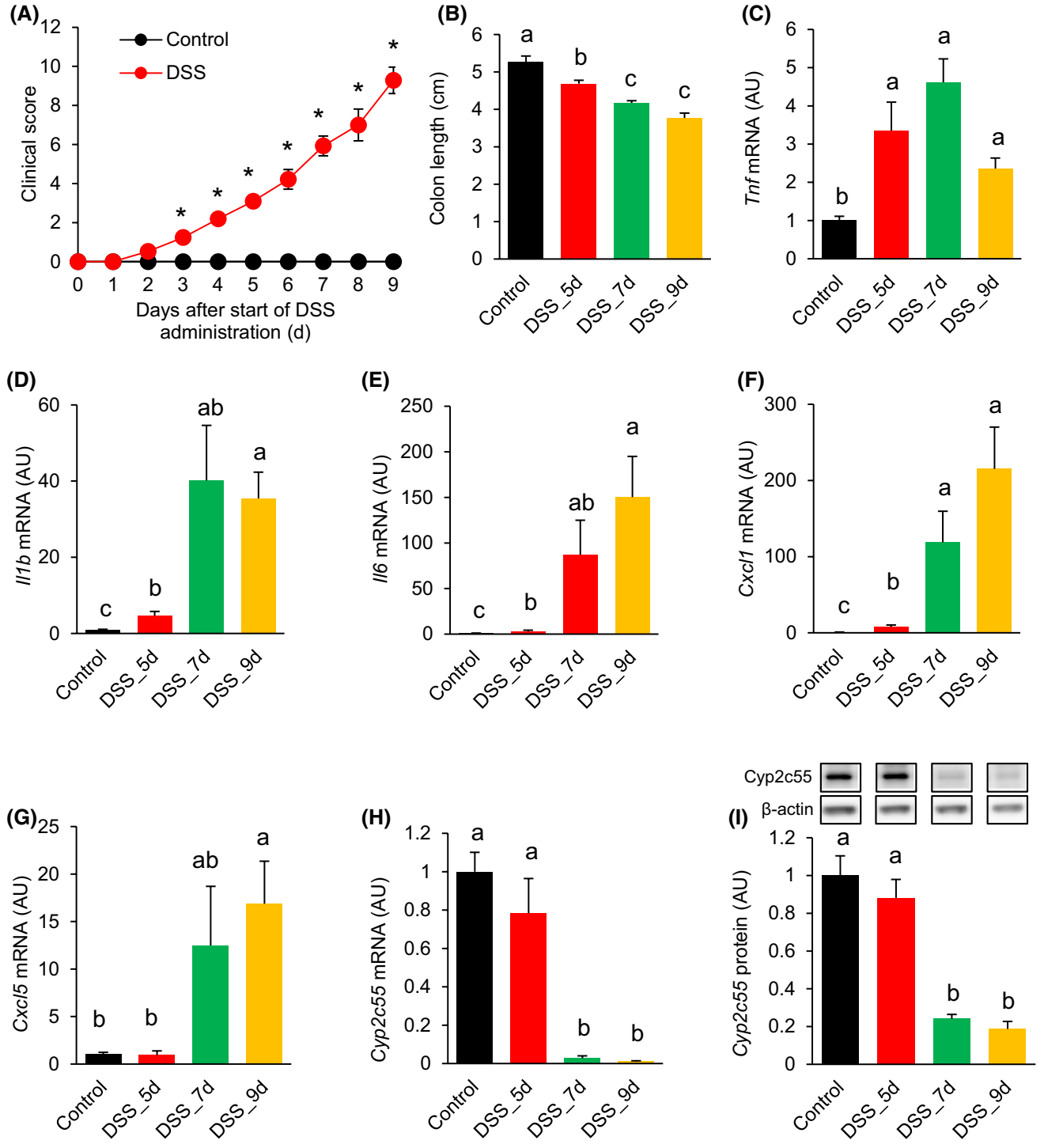


FIGURE 5 Downregulation of the Cyp2c55 expression in colitic mice. (A–I) Mice were administered with dextran sulfate sodium (DSS) for 9 days, and the clinical scores were evaluated every day (A). Colonic tissues were collected 5, 7, and 9 days after the start of the DSS administration, and length of colons was measured (B). The mRNA expression of *Tnf* (C), *Il1b* (D), *Il6* (E), *Cxcl1* (F), and *Cxcl5* (G) in the colonic tissues was analyzed by qRT-PCR analysis. The mRNA (H) and the protein expressions (I) of Cyp2c55 in the colonic tissues were analyzed by qRT-PCR and immunoblot analyses. Data are presented as the mean ± the SEM; $n = 8$. Asterisks indicate significant differences compared with the control mice ($p < .05$). Mean values without a common letter are significantly different ($p < .05$).

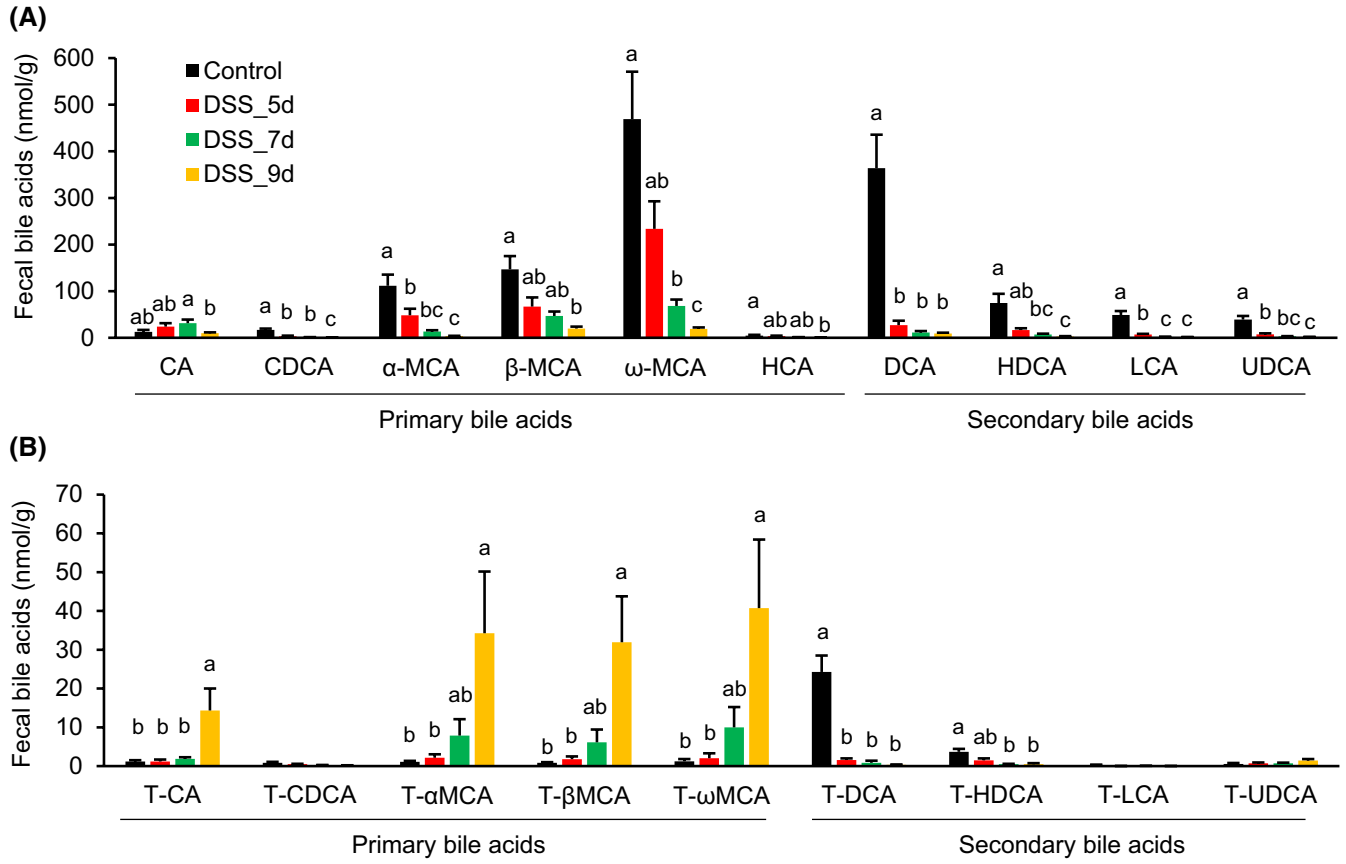


**FIGURE 6** Effect of colitis on the fecal bile acid composition. (A, B) Mice were administered with dextran sulfate sodium (DSS) for 9 days, and feces were collected on days 4, 6, and 8 (one day prior to dissection). The concentrations of unconjugated (A) and taurine (T)-conjugated (B) bile acids (BAs) in feces of control and DSS-administered mice were measured using ultraperformance liquid chromatography–mass spectrometry. Data are presented as the mean ± the SEM; $n = 8$. Asterisks indicate significant differences compared with the control mice ($p < .05$).

### 3.8 | Effect of DSS administration on the HETE production in the colonic tissues

The 12-HETE was higher in the colonic tissues of the DSS_5d and DSS_7d groups than in the control group (Figure S9). The 15-HETE was higher in the DSS_7d group than in the control group. The 5-HETE was unaffected by DSS administration, and neither the 19- nor the 20-HETEs were detected in any group.

### 3.9 | Regulation of the cyp2c55 expression by PXR agonist and inflammatory cytokines in mouse colonoids

Some BAs regulate gene expression through the activation of nuclear receptors such as PXR, CAR, and VDR.[5] In addition, the inflammatory response affects the expression of various genes. To investigate the roles of the nuclear receptors and the inflammatory cytokines in the regulation of the Cyp2c55 expression, mouse colonoids were used in Experiment 4. Among the agonists of three nuclear receptors, PXR, CAR, and VDR, the PXR agonist PCN greatly upregulated the mRNA and the protein expressions of Cyp2c55 in mouse colonoids (Figure 8A,B). In contrast, the inflammatory cytokine mix downregulated the Cyp2c55 expression (Figure 8C,D).

## 4 | DISCUSSION

To establish the mutualistic relationship between the intestinal microbiota and the human host, the intestinal cells must be able to dynamically regulate the gene expression.[24] A deeper comprehension of the underlying molecular mechanisms may potentially pave the way for the development of a novel approach to promote human health. However, the precise nature of these mechanisms remains elusive. In light of the observed downregulation of the Cyp2c55 expression in the colons of germ-free, antibiotics-treated, and DSS-induced colitic mice, we

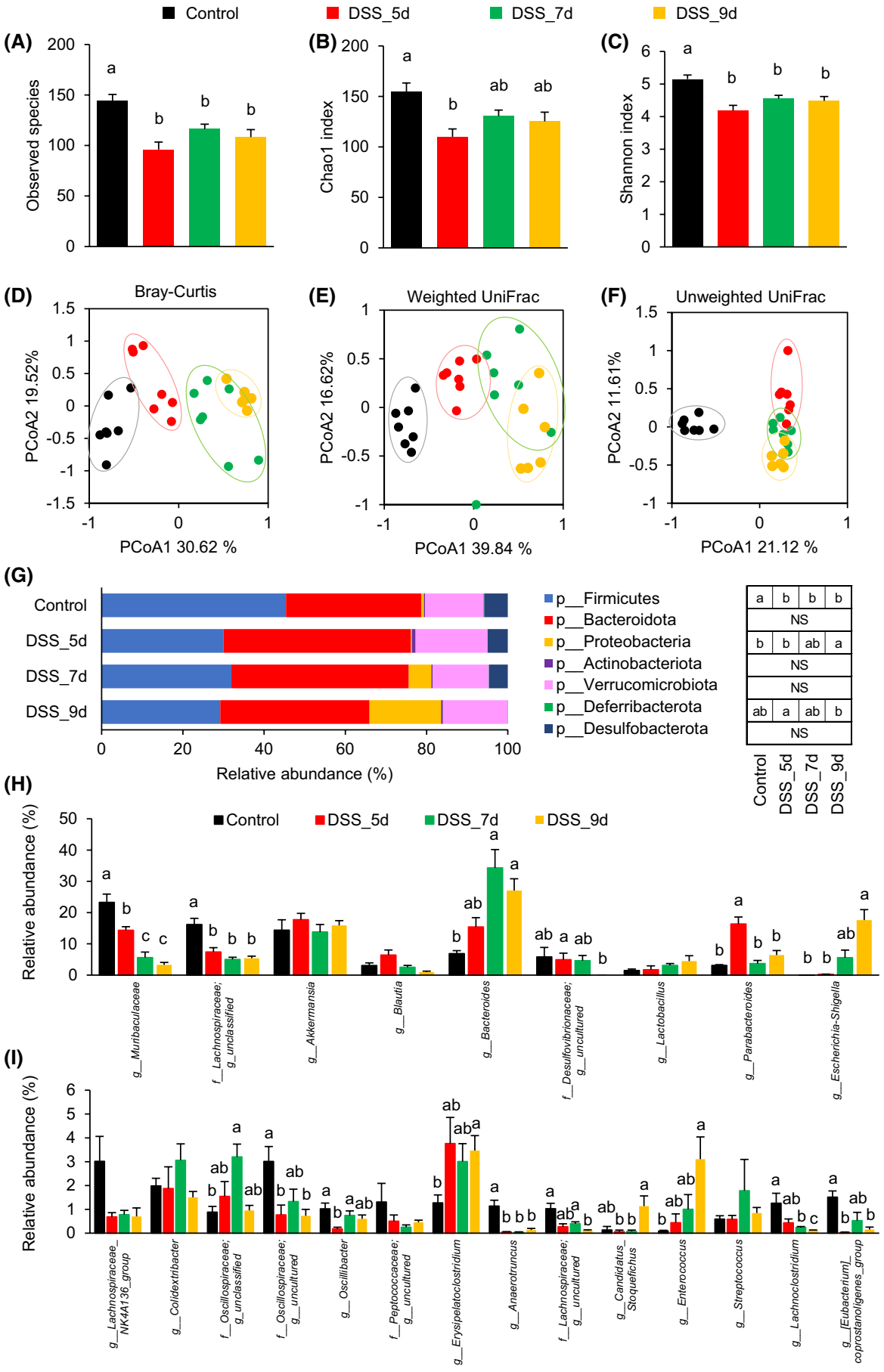
Control
DSS_5d
DSS_7d
DSS_9d
(A)
Observed species
(B)
Chao1 index
(C)
Shannon index
(D)
Bray-Curtis
PCoA2 19.52%
PCoA1 30.62 %
(E)
Weighted UniFrac
PCoA2 16.62%
PCoA1 39.84 %
(F)
Unweighted UniFrac
PCoA2 11.61%
PCoA1 21.12 %
(G)
Relative abundance (%)
p__Firmicutes
p__Bacteroidota
p__Proteobacteria
p__Actinobacteriota
p__Verrucomicrobiota
p__Deferribacterota
p__Desulfobacterota
NS
(H)
Relative abundance (%)
g__Muribaculaceae
f__Lachnospiraceae; g__unclassified
g__Akkermansia
g__Blautia
g__Bacteroides
f__Desulfovibrionaceae; g__uncultured
g__Lactobacillus
g__Parabacteroides
g__Escherichia-Shigella
(I)
Relative abundance (%)
g__Lachnospiraceae_NK4A136_group
g__Colidextribacter
f__Oscillospiraceae; g__unclassified
f__Oscillospiraceae; g__uncultured
g__Oscillibacter
f__Peptococcaceae; g__uncultured
g__Erysipelatoclostridium
g__Anaerotruncus
f__Lachnospiraceae; g__uncultured
g__Candidatus_Stoquefichus
g__Enterococcus
g__Streptococcus
g__Lachnoclostridium
g__[Eubacterium]_coprostanoligenes_group

**FIGURE 7** Effect of colitis on the fecal microbiota composition. (A–I) Mice were administered with dextran sulfate sodium (DSS) for 9 days, and feces were collected on days 4, 6, and 8 (one day prior to dissection). The fecal microbiotas of control and DSS-administered mice were analyzed by 16S rRNA gene sequencing. The number of observed species (A), the Chao1 index (B), and the Shannon evenness (C) in the microbiotas was calculated. A principal coordinate analysis plot of the cecal microbiota was generated based on the Bray–Curtis (D), the weighted UniFrac (E), and the unweighted UniFrac (F) distances using QIIME2. Mean abundances of cecal microbiotas at the phylum level are shown (G). For a better visualization, genera were grouped and divided in those with relative abundances greater than 4% and 1%, respectively (H, I). Data are presented as the mean ± the SEM; $n = 8$. Mean values without a common letter are significantly different ($p < .05$).

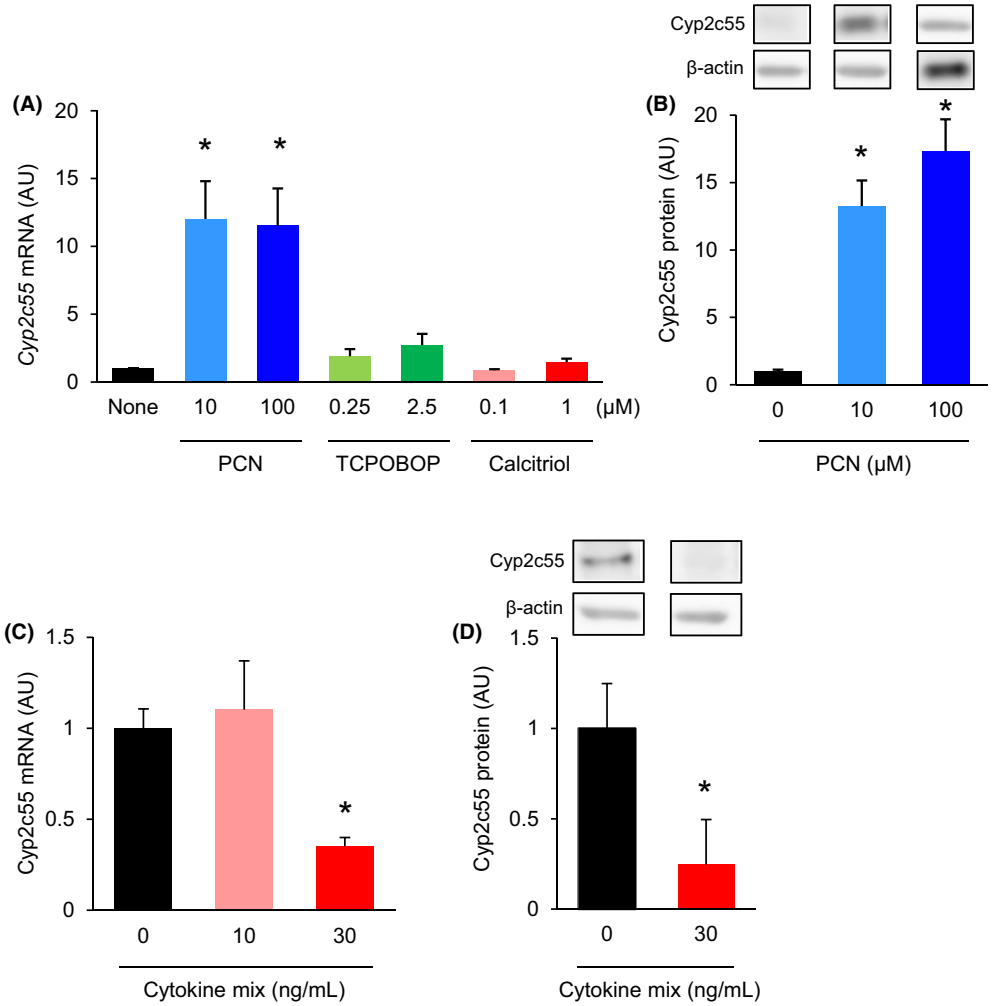


**FIGURE 8** Regulation of the cyp2c55 expression by PXR agonist and inflammatory cytokines in mouse colonoids. (A, B) Mouse colonoids were treated with agonists of PXR [pregnenolone 16α-carbonitrile (PCN)], CAR (TCPOBOP)), and VDR (calcitriol) for 24 h. The mRNA (A) and the protein (B) expressions of CYP2C55 were analyzed by qRT-PCR and immunoblot. (C, D) Mouse colonoids were treated with a cytokine mix (TNF-α, IFN-γ, and IL-1β) for 48 h. The mRNA (C) and the protein (D) expressions of Cyp2c55 were assessed by qRT-PCR and immunoblot analyses. Data are presented as the mean ± the SEM; $n = 4$. Asterisks indicate significant differences compared with the control treatment ($p < .05$).

postulate that the colonic Cyp2c55 expression is a crucial determinant of the mutualistic relationship between the intestinal microbiota and the intestinal homeostasis. Our findings also indicated that the metabolism of BAs by the intestinal microbiota and the inflammatory response are involved in the colonic expression of Cyp2c55. While the physiological function of Cyp2c55 remains largely uncharacterized, our results suggested that Cyp2c55 may represent a novel target for the promotion of intestinal health.

Our findings indicated that the colonic Cyp2c55 expression was significantly reduced at both the mRNA and the protein levels in germ-free and antibiotic-treated mice.

These findings suggested that the Cyp2c55 expression was largely dependent on the intestinal microbiota. This observation was corroborated by the finding that Cyp2c55 was highly expressed in the cecum and the colon, where the intestinal microbiota is densely populated by bacteria, and in contrast with the Cyp2c55 expression in the duodenum and the small intestine, where the bacterial population is sparse. The results of Experiment 2 suggested that vancomycin-sensitive bacteria may play a role in regulating the Cyp2c55 expression. Furthermore, DSS administration induced dysbiosis, which is consistent with previous studies,[25,26] and reduced the colonic Cyp2c55 expression. Due to some genera including *Muribaculaceae*, unclassified *Lachnospiraceae*, *Blautia*, *Lachnoclostridium*, and *Roseburia* showed positive correlations with the mRNA and the protein expressions of Cyp2c55 in Experiments 2 and 3, it can be theorized that these genera may have a potential involvement in the Cyp2c55 expression.

Our results suggested that one of the possible mechanisms underlying the intestinal microbiota-dependent Cyp2c55 expression is the BA-mediated PXR activation. A previous study reported that the hepatic Cyp2c55 expression is induced by the activation of PXR and CAR.[14] Nonetheless, in the present work, an increase in Cyp2c55 in mouse colonoids was induced only by the PXR agonist. Some BAs such as LCA, DCA, and CA are known to be ligands of PXR, which regulate cellular functions.[27,28] Together with the results of the correlation analyses carried out in the present study, this evidence indicated that these three BAs, at least in part, contributed to the colonic Cyp2c55 expression. Taurine-conjugated PBAs secreted from liver into the duodenum are predominantly reabsorbed in the terminal ileum. Any small portion of taurine-conjugated PBAs (~5%) that escapes from reabsorption is deconjugated by the bacterial bile salt hydrolase (BSH) activity and transformed to SBA by the bacterial 7α-dehydroxylase activity. DCA and LCA positively correlated with *Muribaculaceae*, unclassified *Lachnospiraceae*, *Blautia*, *Lachnoclostridium*, and *Roseburia* (Figures S10 and S11). Furthermore, it has been reported that *Muribaculaceae*, some genera of the *Lachnospiraceae* family, and *Lachnoclostridium* possess the BSH and that some genera of the *Lachnosiraceae* family and *Lachnoclostridium* possess 7α-dehydroxylase.[29,30] Therefore, it is likely that these BSH- and 7α-dehydroxylase-possessing bacterial genera are involved in the production of unconjugated DCA and LCA, resulting in the upregulation of colonic Cyp2c55.

It was hypothesized that the inflammatory signaling as well as the BA metabolism may contribute to the downregulation of the colonic Cyp2c55 expression in DSS-induced colitic mice. This hypothesis seems to have been corroborated by the present study, as it was shown that the inflammatory cytokines reduced the Cyp2c55 expression in mouse colonoids. Previous work indicated that inflammatory cytokines can affect the expression of numerous genes that are crucial for maintaining the intestinal homeostasis, ultimately leading to tissue destruction. For instance, the inflammatory signaling initiated by TNFα, IFNγ, IL-1β, and IL-6 has been shown to impair the structural integrity of tight junctions and the production of mucins.[31,32] Further investigation is necessary to fully elucidate the precise mechanism by which cytokines reduce the Cyp2c55 expression.

The findings of the present study indicated that the colonic Cyp2c55 expression was associated with the BA metabolism and the inflammatory conditions. However, it is worth noting that the present work had some limitations. Although an in vitro study has characterized Cyp2c55 as an enzyme that catalyzes the 19-HETE synthesis,[10] in the present work, the 19-HETE was not detected in the mouse colon, where Cyp2c55 is highly expressed. However, it should be noted that, to date, no study has reported the presence of the 19-HETE in the intestinal tissues. Nonetheless, in accordance with the findings of previous studies,[33,34] we were able to successfully detect the presence of the 5-, 12-, and 15-HETEs in the colon. Further research is required to elucidate the physiological role of Cyp2c55. It is possible, however, that other microbial metabolites, in addition to BAs, may be involved in the colonic expression of Cyp2c55. For example, the tryptophan-derived microbial metabolites indole 3-propionic and 3-acetic acids have been identified as agonists of PXR.[35] It is foreseeable that the precise mechanisms underlying the microbiota-dependent expression of Cyp2c55 will be elucidated in future studies.

The present study demonstrated that Cyp2c55 is highly expressed in the colonic epithelial cells of mice in a microbiota-dependent manner. The underlying mechanism seems to involve a BA-mediated PXR activation. Furthermore, the colonic expression of Cyp2c55 is also subject to regulation by the inflammatory response. While the physiological function of Cyp2c55 remains largely unidentified, our findings suggested that Cyp2c55 may play a role in the mutualistic interaction between the intestinal microbiota and the intestinal homeostasis.

## AUTHOR CONTRIBUTIONS

Adrian Hilman, Tetsu Sato, and Takuya Suzuki conceived and designed the research. Adrian Hilman, Tetsu Sato, Bambang Dwi Wijatniko, So Fujimura, Katsushi Nakamura, and Ryo Inoue performed the research and acquired the data. All authors analyzed and interpreted

the data. All authors were involved in drafting and revising the manuscript.

## ACKNOWLEDGMENTS

This work was supported in part by the Natural Science Center for Basic Research and Development (NBARD-00057). This study was partially supported JSPS Kakenhi (Grant Number 22H03512) and the Tojuro Iijima Foundation for Food Science and Technology.

## CONFLICT OF INTEREST STATEMENT

The authors have no affiliation with any organization with a direct or indirect financial interest in the subject matter discussed in the manuscript. The authors declare no competing financial interests.

## DATA AVAILABILITY STATEMENT

Data will be made available on request.

## ORCID

*Adrian Hilman* https://orcid.org/0000-0002-5441-9099
*Bambang Dwi Wijatniko* https://orcid.org/0000-0002-2963-2568
*Hiroto Miura* https://orcid.org/0000-0003-1736-4428
*Ken Iwatsuki* https://orcid.org/0000-0003-4130-2964
*Ryo Inoue* https://orcid.org/0000-0002-7233-366X
*Takuya Suzuki* https://orcid.org/0000-0003-3709-543X

## REFERENCES

1. Kim S, Seo SU, Kweon MN. Gut microbiota-derived metabolites tune host homeostasis fate. *Semin Immunopathol*. 2024;46:2.
2. Hayes CL, Dong J, Galipeau HJ, et al. Commensal microbiota induces colonic barrier structure and functions that contribute to homeostasis. *Sci Rep*. 2018;8:14184.
3. Ekstedt N, Jamioł-Milc D, Pieczyńska J. Importance of gut microbiota in patients with inflammatory bowel disease. *Nutrients*. 2024;16:2092.
4. Biazzo M, Deidda G. Fecal microbiota transplantation as new therapeutic avenue for human diseases. *J Clin Med*. 2022;11:4119.
5. Lee MH, Nuccio SP, Mohanty I, et al. How bile acids and the microbiota interact to shape host immunity. *Nat Rev Immunol*. 2024.
6. Molinaro A, Wahlström A, Marschall HU. Role of bile acids in metabolic control. *Trends Endocrinol Metab*. 2018;29:31-41.
7. Su X, Gao Y, Yang R. Gut microbiota derived bile acid metabolites maintain the homeostasis of gut and systemic immunity. *Front Immunol*. 2023;14:1127743.
8. Campbell C, McKenney PT, Konstantinovsky D, et al. Bacterial metabolism of bile acids promotes generation of peripheral regulatory T cells. *Nature*. 2020;581:475-479.
9. Thelen K, Dressman JB. Cytochrome P450-mediated metabolism in the human gut wall. *J Pharm Pharmacol*. 2009;61:541-558.
10. Wang H, Zhao Y, Bradbury JA, et al. Cloning, expression, and characterization of three new mouse cytochrome p450 enzymes and partial characterization of their fatty acid oxidation activities. *Mol Pharmacol*. 2004;65:1148-1158.
11. Özen N, Nasırcılar Ülker S, Ülker P, et al. Effect of 20-HETE inhibition on L-NAME-induced hypertension in rats. *Clin Exp Hypertens*. 2018;40:292-302.
12. Pochard C, Coquenlorge S, Jaulin J, et al. Defects in 15-HETE production and control of epithelial permeability by human enteric glial cells from patients with Crohn's disease. *Gastroenterology*. 2016;150:168-180.
13. Graves JP, Gruzdev A, Bradbury JA, DeGraff LM, Edin ML, Zeldin DC. Characterization of the tissue distribution of the mouse Cyp2c subfamily by quantitative PCR analysis. *Drug Metab Dispos*. 2017;45:807-816.
14. Konno Y, Kamino H, Moore R, et al. The nuclear receptors constitutive active/androstane receptor and pregnane x receptor activate the Cyp2c55 gene in mouse liver. *Drug Metab Dispos*. 2010;38:1177-1182.
15. Ogata M, Ogita T, Tari H, Arakawa T, Suzuki T. Supplemental psyllium fibre regulates the intestinal barrier and inflammation in normal and colitic mice. *Br J Nutr*. 2017;118:661-672.
16. Vonk AM, van Mourik P, Ramalho AS, et al. Protocol for application, standardization and validation of the Forskolin-induced swelling assay in cystic fibrosis human colon organoids. *STAR Protoc*. 2020;1:100019.
17. Ishii Y, Matsunaga T, Yasui T, et al. Supplemental psyllium fiber increases antimicrobial proteins via the tuft cell-ILC2 circuit and type II immune response in the mouse small intestine. *Forum Nutr*. 2024;4:307-322.
18. Hagio M, Matsumoto M, Fukushima M, Hara H, Ishizuka S. Improved analysis of bile acids in tissues and intestinal contents of rats using LC/ESI-MS. *J Lipid Res*. 2009;50:173-180.
19. Shaik JS, Miller TM, Graham SH, Manole MD, Poloyac SM. Rapid and simultaneous quantitation of prostanoids by UPLC-MS/MS in rat brain. *J Chromatogr B Analyt Technol Biomed Life Sci*. 2014;945-946:207-216.
20. Hayashi A, Mikami Y, Miyamoto K, et al. Intestinal dysbiosis and biotin deprivation induce alopecia through overgrowth of lactobacillus murinus in mice. *Cell Rep*. 2017;20:1513-1524.
21. Klindworth A, Pruesse E, Schweer T, et al. Evaluation of general 16S ribosomal RNA gene PCR primers for classical and next-generation sequencing-based diversity studies. *Nucleic Acids Res*. 2013;41:e1.
22. Owen BM, Milona A, van Mil S, et al. Intestinal detoxification limits the activation of hepatic pregnane X receptor by lithocholic acid. *Drug Metab Dispos*. 2010;38:143-149.
23. Hung TV, Suzuki T. Dietary fermentable fiber reduces intestinal barrier defects and inflammation in Colitic mice. *J Nutr*. 2016;146:1970-1979.
24. Lu L, Yu Y, Guo Y, Wang Y, Chang EB, Claud EC. Transcriptional modulation of intestinal innate defense/inflammation genes by preterm infant microbiota in a humanized gnotobiotic mouse model. *PLoS One*. 2015;10:e0124504.
25. Llewellyn SR, Britton GJ, Contijoch EJ, et al. Interactions between diet and the intestinal microbiota alter intestinal permeability and colitis severity in mice. *Gastroenterology*. 2018;154:1037-1046.e1032.
26. Ai L, Ren Y, Zhu M, et al. Synbindin restrains proinflammatory macrophage activation against microbiota and mucosal inflammation during colitis. *Gut*. 2021;70:2261-2272.

27. Hang S, Paik D, Yao L, et al. Bile acid metabolites control T(H)17 and T(reg) cell differentiation. *Nature*. 2019;576:143-148.
28. Carazo A, Hyrsova L, Dusek J, et al. Acetylated deoxycholic (DCA) and cholic (CA) acids are potent ligands of pregnane X (PXR) receptor. *Toxicol Lett*. 2017;265:86-96.
29. Song Z, Cai Y, Lao X, et al. Taxonomic profiling and populational patterns of bacterial bile salt hydrolase (BSH) genes based on worldwide human gut microbiome. *Microbiome*. 2019;7:9.
30. Vital M, Rud T, Rath S, Pieper DH, Schlüter D. Diversity of bacteria exhibiting bile acid-inducible 7α-dehydroxylation genes in the human gut. *Comput Struct Biotechnol J*. 2019;17:1016-1019.
31. Suzuki T, Yoshinaga N, Tanabe S. Interleukin-6 (IL-6) regulates claudin-2 expression and tight junction permeability in intestinal epithelium. *J Biol Chem*. 2011;286:31263-31271.
32. Graham WV, He W, Marchiando AM, et al. Intracellular MLCK1 diversion reverses barrier loss to restore mucosal homeostasis. *Nat Med*. 2019;25:690-700.
33. Kroschwald S, Chiu CY, Heydeck D, et al. Female mice carrying a defective Alox15 gene are protected from experimental colitis via sustained maintenance of the intestinal epithelial barrier function. *Biochim Biophys Acta Mol Cell Biol Lipids*. 2018;1863:866-880.
34. Austin Pickens C, Yin Z, Sordillo LM, Fenton JI. Arachidonic acid-derived hydroxyeicosatetraenoic acids are positively associated with colon polyps in adult males: a cross-sectional study. *Sci Rep*. 2019;9:12033.
35. Venkatesh M, Mukherjee S, Wang H, et al. Symbiotic bacterial metabolites regulate gastrointestinal barrier function via the xenobiotic sensor PXR and toll-like receptor 4. *Immunity*. 2014;41:296-310.

## SUPPORTING INFORMATION

Additional supporting information can be found online in the Supporting Information section at the end of this article.

**How to cite this article:** Hilman A, Sato T, Wijatniko BD, et al. The expression of intestinal Cyp2c55 is regulated by the microbiota and inflammation. *The FASEB Journal*. 2024;38:e70117. doi:10.1096/fj.202401807R